Fischer-Tropsch Synthesis: Effect of CO Conversion on CH_4 and Oxygenate Selectivities over Precipitated Fe-K Catalysts

Wenping Ma,[1] Wilson D. Shafer,[1,2] Gary Jacobs,[1,3] Jia Yang,[1,4] Dennis E. Sparks,[1] Hussein H. Hamdeh,[5] and Burtron H. Davis[1 *]

[1]University of Kentucky, Center for Applied Energy Research, Lexington, KY 40511, USA.
[2]Health and Science Department, Asbury University, Wilmore, KY 40390
[3]Chemical Engineering Program – Department of Biomedical Engineering & Department of Mechanical Engineering, University of San Antonio, San Antonio, TX 78249
[4] Department of Chemical Engineering, Norwegian University of Science and Technology, Trondheim, Norway
[5] Department of Physics, Wichita State University, Wichita, KS 67260

Abstract

The explanation for CH_4 selectivity for iron based Fischer-Tropsch catalysts in the low conversion region (i.e., < 50%) remains elusive. In this contribution, the CO conversion effect was carefully examined over four K promoted Fe catalysts (100 Fe/5.1Si/2Cu/ x K, where x = 1 – 5) over a wide range of CO conversion (i.e., 4 - 85%). Moreover, the effect of CO conversion on oxygenate selectivity of the Fe-K catalysts was carefully studied as well. The change in CH_4 selectivity with CO conversion was found to resemble asymmetric "V" shaped curves, with the minimum values occurring at approximately 50% CO conversion. Adding greater than x = 2 K significantly alleviated the CO conversion effect which was attributed to the high K loading greatly decreasing the surface H coverage while improving CO adsorption. The unique CH_4 selectivity trend suggests a complicated CH_4 formation process that results from different aspects of the catalyst (i.e., chain growth and hydrogenation rates), and process conditions. Oxygenate selectivity was in the range of 0.7 to 2.8% and varied with the CO conversion and K loading. The addition of K up to x = 3 was found to promote oxygenate formation and chain growth. The

* Corresponding author: tel: +1 (859) 257-0251; email: burtron.davis@uky.edu

overall oxygenate distribution up to C_{17} follows an Anderson-Schulz Flory (ASF) distribution, with ethanol being the dominant oxygenate. Mechanisms of oxygenate formation different from that of hydrocarbon formation (e.g., CO insertion versus CO dissociation) were proposed to explain the experimental results.

Keywords: Fischer-Tropsch synthesis; iron catalysts; CO conversion effect; CH_4 selectivity oxygenate selectivity; K promoter

Introduction

Despite the fact that the Fischer-Tropsch synthesis (FTS) has been studied extensively studied the past nine decades [1-17], the influence of process conditions, such as the CO conversion, on hydrocarbon (HC) selectivity for iron based catalysts is still not well established. Significant advances in XTL (X = coal, natural gas (NG), biomass, and CO_2) technology have been made and many XTL plants have been commissioned worldwide in South Africa, Nigeria, Malaysia, Qatar, and China [1-9]. Considering this rapid industrial growth, the issue of variation of methane selectivity with conversion becomes increasingly important in order to optimize heavier HC productivity and limit Greenhouse Gas emissions.

The CO conversion effect on CH_4 formation for cobalt catalysts has been studied in a systematic manner and consistent conclusions have been drawn [10-13]; the CH_4 selectivity decreases monotonously with increasing CO conversion up to 80%. This has been explained by a negative kinetic effect of water on CH_4 formation during FTS [18]. Unlike cobalt based catalysts, the effect of CO conversion on iron based FTS catalysts has not yet been thoroughly studied; this is in part because it is a more complex reaction system in which the water gas shift (WGS) reaction is significantly involved. In several previous promoter effect studies [14-16] using

continuously stirred tank reactors (CSTR), the findings were seemingly inconsistent and therefore require further investigation. Raje et al. [14] reported that CH_4 selectivity increased monotonically from 10 to 15% with increasing CO conversion from 10 to 90% at 270 ^oC, 1.3 MPa and $H_2/CO = 0.67$ for a 100 Fe/4.4 Si/0.5K catalyst; on the other hand, a virtually negligible change in CH_4 selectivity (i.e., ~5%) below 50% CO conversion was reported in subsequent K (0.36 to 2.2) and Cu (0.1-2.0) promoter effect studies [15,16] as well as in a recent review [17]. Therefore, there is no affirmative conclusion on the effect of CO conversion on CH_4 formation of iron-based catalyst; furthermore, how promoters impact the CO conversion effect remains unclear.

Oxygenates are produced simultaneously with hydrocarbons on iron based FTS catalysts. The oxygenate selectivity of an iron catalyst is generally small (i.e., less than x = 3); however, this is not negligible, especially considering the production capacity of a commercial plant. Thus, determining the oxygenate selectivity and distribution is of great importance from an industrial viewpoint. Ma et al. [19] reported that about 3% of converted carbon went to water soluble oxygenates on x = 1 to 2 K promoted Fe/AC catalysts and K promoter was found to inhibit oxygenate formation at 260-300 ^oC and 2 MPa. Yang et al. [20] reported quite high oxygenate selectivities (i.e., 7-31%) on x = 0.2 to 3 K promoted Fe-Mn catalysts under the conditions: 270-300 ^oC, 2.50 MPa, and $H_2/CO = 2.0$. The effects of CO conversion on oxygenate selectivity and distribution over iron based catalysts have not been systemically studied.

Consequently, the current study was undertaken to carefully investigate the effect of CO conversion on CH_4 selectivity and selectivity for oxygenates and hydrocarbons for K promoted Fe catalysts using a 1L CSTR. The process conditions 260-270 ^oC, $H_2/CO = 0.67$ and 1.3 MPa were employed. The upper limit of CO conversion was 85% while the lower limit of CO

conversion was 4%, a conversion that is low enough to give new insight into the CO conversion impact on selectivity. The results for all catalysts were reproduced in the same run as well as in separate runs by repeating the same conditions. Different mechanisms for oxygenate and hydrocarbon formation were proposed to interpret the selectivity changes of the catalysts.

Experimental

Catalyst preparation

Four potassium promoted iron catalysts, 100 Fe/5.1Si/2Cu/ x K, where x = 1, 2, 3 and 5, were used to investigate the CO conversion and K loading effects. To prepare the catalysts, a base Fe catalyst (100Fe/5.1Si) was first prepared using a precipitation method. Details of catalyst preparation can be found elsewhere [21-22]. The 100Fe/5.1Si/2Cu/xK catalyst was prepared by sequential impregnation of appropriate amounts of Cu ($Cu(NO_3)_2 \bullet 2.5\ H_2O$, 99.9% purity) and K ($KNO_3$, 99.9% purity) containing solutions. Between each step, the catalyst was dried under vacuum in a rotary evaporator at 80°C and the temperature was then slowly increased to 95 °C. After the impregnation/drying step, the catalyst was calcined under an air flow at 350 °C for 4 h and sieved to a size range of 45-90 μm. ICP results of the four Fe-K catalysts are provided in Table 1. The experimental compositions of all catalysts are consistent with the nominal compositions. The BET surface areas of the Fe-K catalysts were ~110 m^2/g. Note that the atomic ratio of Cu in all iron catalysts (i.e., 100Fe/5.1Si/2Cu/xK) was maintained at 2 to ensure that the added Cu promoter did not affect a determination of the K loading effect in this study; it has been reported that changes in Cu loading alter CH_4 selectivity to a certain extent by presenting either the Cu^0 or the Cu^{+1} state under syngas activation, respectively [23]. The 100 Fe/5.1Si/2Cu/1K, /2 K, /3K and /5K catalysts are abbreviated as 1K, 2K, 3K and 5K catalysts, respectively.

Catalyst Testing

The FTS reaction for the iron catalysts (45-90 μm) was carried out using a 1-L CSTR. Durasyn-164 C_{30} oil (~300 g) was used as the startup solvent. The iron catalysts were charged to the reactor for *in-situ* reduction by CO at 270 ^{o}C and 1 atm for 24 h. After activation, the iron catalysts were tested at 260-270 ^{o}C, 1.3 MPa, $H_2/CO = 0.67$ over a wide range of CO conversion (i.e., 4–85%). Steady state was achieved after 120 h. To ensure accuracy of the data, the process conditions were repeated within the same run or by using a different run. The results were reproduced and the mass balance period for each set of conditions lasted approximately 8–16 h. The total and elemental closures were generally 100 ± 2%. The hydrogen and carbon monoxide conversions (X_i), CH_4 and oxygenate selectivities, partial pressures of hydrogen, carbon monoxide and water ($P_{H_2}, P_{CO}, P_{H_2O}$) used in this paper are defined by the following formulas:

$$X_i, \% = 100* (N_{i,\,in} - N_{i,out})/N_{i,\,in} \quad (1)$$

$$CH_4 \text{ selectivity}, \% = 100 * N_{CH_4}/(N_{CO,\,in} - N_{CO,out} - N_{CO_2}) \quad (2)$$

$$\text{Oxygenate selectivity}, \% = 100 * N_{oxy}/(N_{oxy} + N_{HC}) \quad (3)$$

$$P_{H_2} = P_{H_2}{}^{0}\left(1 - X_{H_2}\right) \quad (4)$$

$$P_{CO} = P_{CO}{}^{0}(1 - X_{CO}) \quad (5)$$

$$P_{H_2O} = P_{H_2}{}^{0} N_{H_2O} N_{H_2}{}^{0} \quad (6)$$

where i refers to CO or H_2, $N_{i,\,in}$ and $N_{i\,out}$ are the molar flow rates of CO or H_2 at the inlet and outlet, respectively; N_{CH_4} and N_{CO_2} are the molar formation rates of CH_4 and CO_2, respectively; N_{oxy} and N_{HC} are the molar formation rates of oxygenate and hydrocarbon, respectively; $P_{H_2}{}^{0}$ and

P_{CO}^0 are inlet partial pressures of H_2 and CO; and N_{H_2O} and $N_{H_2}{}^0$ are the molar formation rate of water and the inlet molar flow rate of H_2, respectively.

Analysis of FT products.

Quantification of the oil products was done using a 6890 Agilent (Santa Clara, CA) GC with flame ionization detector (FID). No sample preparation was needed before injection of the oil sample on the GC column. One microliter of sample was injected on an Agilent JW Scientific DB-5 GC Column (Agilent, Santa Clara) at 35 ^oC and 8 psi with a 1.5 ml/min split flow.

Aqueous samples were injected onto the SRI8610 GC with thermal conductivity detector (TCD) and packed (1/8" x 6m Porapak) column at 20 psig, and 100 °C, and also to an 8610C SRI GC using the same column and method. The water component was identified by matching retention times of known standards. Calibration of the SRI8610 GC was performed by injecting a standard solution containing 91.6% water, 2.0% C_1-OH, 3.7% C_2-OH, 1.9% C_3-OH and 0.8% C_4-OH to quantify the water product composition.

Gas from the CSTR was analyzed online with a Hewlett-Packard Quad Series Micro GC (MicroGC 3000 from Agilent) specifically used as a refinery gas analyzer (RGA). This GC has four columns that run in parallel (MolSieve 10 m 5A, Plot U (PPU) 8 m, Alumina 10 m, OV-1 10 m). Two pumps in the GC allow the same volume of sample to be injected into the four columns (being held at a constant temperature and pressure), quickly separating specific compounds in each column.

Specific oxygenates for all the runs were only identified (i.e., not quantified) using an Agilent 5975N MSD directly connected to a 6890 GC using the same GC conditions and column as the 6890 Agilent GC-FID. By doing this, the peaks observed in the chromatographs could be matched between the FID and MSD, where the retention times and patterns of specific

compounds are the same. Thus, this allows for specific product verification (by the MSD) and quantification (by FID) for as many of the FT products as possible. Note that calibration of each component detected by the oil GC FID was not possible. Unit response factors for each hydrocarbon product (C_4-C_{35}) were applied; alcohol components were suppressed in the FID signal, and thus the response factors of 0.46-0.86 taken from reference [24] were used to calculate oxygenate composition (C_4-C_{17}) in the oil phase.

Catalyst characterization

Inductively coupled plasma optical emission spectrometry (ICP-OES) was used to analyze Fe-K catalyst composition. Meanwhile, powder X-ray diffraction (XRD) was carried out for the reduced Fe-K catalysts at room temperature using a Rigaku Diffractometer (DMAX-B) operating with Cu Kα radiation (1.54 Å). This was used to determine if size of iron carbide changed greatly with K loading. Before the XRD experiment, the Fe-K samples were reduced at the same conditions (270 ^{o}C for 24 h by CO) as used for the FTS reaction tests followed, with the exception that they were passivated using 1%O_2 in nitrogen.

Mössbauer spectroscopy measurements were conducted in transmission mode, with a ^{57}Fe source mounted in a standard constant acceleration velocity transducer, in order to find out whether iron phases change significantly with CO conversion. The used 3K Fe catalysts, in slurry form, were collected after separate runs at a high (i.e., 80%) or low (i.e., 30%) conversion for 192 h. The samples were placed in a copper holder and mounted near the finger of a vibration-free closed-cycle refrigerator which provided temperatures as low as 20 K. Structural analysis of the samples was performed by least-squares fitting of the Mössbauer spectra to a summation of hyperfine sextets. The least squares fitting procedure employed user-defined functions within the Peak Fit program. The parameters for each sextet in the fit consisted of the

position, width and height of the first peak, the hyperfine magnetic field, and the quadrupole electric field. These parameters were allowed to vary freely to obtain the best fit of the experimental data. Errors in the determined percentages of Fe are about ±3 % for well-resolved spectra; in those that contain several iron oxide and carbide phases, the uncertainty increases with the complexity of the spectrum (i.e., depending on the degree of overlap and the weakness of the signal).

Results and Discussion

Effects of K loading and CO conversion on CH_4 selectivity.

CH_4 selectivity for the K promoted iron based catalysts is generally low (i.e., 2-6%) at typical FTS conditions due to the significant role of K promoter in promoting CO dissociation and chain growth. Table 2 gives CH_4 selectivities at 250 to 270 ^oC over the four Fe-K catalysts. Apparently, both the 1K and 3K Fe catalysts displayed low CH_4 selectivity within a narrow range over the temperature range 250-270 ^oC. For example, between 75 and 80% CO conversion, CH_4 selectivity varied between 5.1 and 5.6% for the 1K catalyst and between 2.3 and 3.3% for the 3K catalyst. Therefore, the CH_4 selectivity of the Fe-K catalysts is not very sensitive to temperature. At 260 ^oC, CH_4 selectivity decreased from 5.3 to 2.1% with increasing K from x = 1 to 5. This strongly suggests a role played by K in enhancing CO dissociation and promoting chain growth for iron catalysts.

The CO conversion effect on CH_4 selectivity in the low CO conversion range of 10-15% was examined in previous studies [14-16]. In this contribution, the four Fe-K catalysts (i.e., 1K, 2K, 3K and 5K) were tested and CO conversion levels as low as 4% were used to obtain a more pronounced CO conversion effect on selectivity and the impact of K loading. All data were

reproduced in the same run or in separate runs (reproduced results not shown), demonstrating reliability of the data. Note that the K promoter also affects activity of iron catalyst, possibly through its changing degrees of iron reduction, dispersion and iron carburation, but this is not the scope of this study. More info about the K effect of Fe catalyst activity can be found elsewhere [19-21, 26].

The changes in CH_4 selectivity with CO conversion over 1K, and 2K, 3K and 5K catalysts were measured at 270 ^oC and 260 ^oC, respectively, and the results are displayed in Figure 1. For the 1K catalyst, a well-defined parabolic shaped curve was obtained, which indicates a prominent CO conversion effect on CH_4 selectivity for the iron catalyst. In particular, the CO conversion effect was quite distinct in the lower CO conversion range of 4.5 to 50%. CH_4 selectivity was as high as 9.0% at a CO conversion of 4.5% but at a conversion of 50% it decreased to 4.6%. Interestingly, CH_4 selectivity tends to increase after this point, reaching 6% at 85% CO conversion. A similar parabolic shaped CH_4 selectivity versus CO conversion curve was also observed over the 2K and 3K catalysts with the minimum occurring at about the same conversion, 50% (Figure 1). However, compared to Figure 1 (top), a notable difference is that CH_4 selectivity of the 2K and 3K catalysts was much lower (i.e., 3-4%, and 2.6 -3.5% for the 2K and 3K catalysts, respectively) compared to the 1K catalyst, and the degree of change was smaller as the conversion increased from 4 to 85%, respectively. When K was further increased to x = 5, CH_4 selectivity was decreased further to ~1.9% and the degree of change became even smaller, which indicates that the conversion effect can be virtually neglected in the case of the 5K catalyst. Therefore, CO conversion has a distinct effect on CH_4 selectivity for the K promoted iron catalysts, and it was dramatically suppressed by increasing to a 5K loading, where the CO conversion effect was almost eliminated. Note that Cu was present in all four Fe-K

catalysts; however the Cu promoter is not a dominant reason for the CO conversion effect with diffeent Fe-K catalysts. Rather, the K loading played the major role. To confirm this conclusion, Table 3 lists the FTS data of 100Fe/5.1Si/1.3K with and without Cu. Cu had very little effect on various hydrocarbon selectivities for the 100Fe/5.1Si/1.3K catalyst at 75% and 42-48% CO conversion levels. This is consistant with Cu promoter effect studies of Fe-K catalysts [25, 26].

The asymmetric V-shaped CH_4 selectivity versus CO conversion curves for the Fe-K catalysts are presumed to be governered by the process conditions and the nature of the Fe-K catalyst. In the low CO conversion region (i.e., < 50%), the H_2/CO ratio shown in Figure 2, which was adjusted by the WGS reaction, decreased slightly from 0.61 to 0.55 for the 1K and 2K catalysts, and this contributes in part to the decrease in CH_4 selectivity. For the 3K and 5K catalysts, the H_2/CO ratio in the low conversion region remained nearly constant (i.e., 0.65–0.67) due to the promoting effect of K on the WGS reaction, which in turn adjusts to a greater extent the P_{H_2}. This implies that the decrease in, or relatively unchanged, CH_4 selectivity with CO conversion on the two catalysts was less affected by the change in process conditions, but rather that the K promoter provided a greater role in changing CO or H_2 adsorption and chain growth, which is consistent with many studies regarding the role of K on the adsorption of H_2 and CO on iron catalysts (e.g., K increases CO chemisorption and increases Fe-C bond strength [26-31], and K decreases H chemisorption and weakens Fe-H bond strength on iron based catalysts [26-28,31]). This conclusion is further evidenced by the significant decrease in the CO conversion effect with increasing K loading. For example, the percentage change in the CH_4 selectivity (100 x (CH_4 selectivity at t_0 - CH_4 selectivity at t_1)/CH_4 selectivity at t_0) in the low conversion region decreased greatly from 49 to 3% as the K loading increased from 1 to 5% (Table 4). The results are again consistent with previous studies [27-31] on the role of K in strengthening CO

adsorption and weakening H_2 adsorption, respectively, with K promoting chain growth [19,26] on iron catalysts resulting in lower CH_4 selectivity and lower extents of change on the higher K loading catalysts. At the high CO conversion level (i.e., > 50%), the WGS activity of the Fe-K catalysts was enhanced significantly, which led to a precipitous increase in the H_2/CO ratio (0.6 to 0.88 for 1 K, 0.67 to 1.09 for 2-5 K in Figure 2) with increasing CO conversion; this reversed the CH_4 selectivity trend such that it increased with further increases in CO conversion. Table 4 shows that CH_4 selectivity had similar percentage increases (i.e., 30–33%), which was accompanied by different extents of increase in the H_2/CO ratio for the 1-3 K catalysts (i.e., greater change in H_2/CO ratio on 2–3 K than 1 K), while it was only 20% for the 5 K catalyst. This result further demonstrates that higher K loading weakens the CO conversion effect at the high CO conversion range by promoting CO adsorption and suppressing H_2 adsorption.

From the kinetic point of view, CH_4 selectivity is a function of the coverages of surface species CH_3, C or CH if assuming CH_4 is formed through the hydrogenation of surface CH_3 groups (CH_3-s + H-s -> CH_4 +2s, where s is an active site):

$$s_{CH_4} = r_{CH_4}/r_{FT} = k_M[CH_3]/k_{FT}[x] \quad (7)$$

Where k_M, k_{FT} are rate constants for the CH_4 formation and overall FT reaction, x can be a species such as C, CH, CH_2, CO or CHO, etc. in terms of surface carbide (also known as alkyl or CH_2 insertion) [32,33], CO insertion [34,35], enol [36,37], alkenyl [38], or H-assisted CO dissociation (HCO-s + H_2 (or H-s) –> CH_2-s) [39-42] mechanisms. Since the surface [CH_3] is associated with the surface [H] and chain growth probability α_1, [CH_3] = α_1 [H], eq (7) can be rewritten as follows:

$$s_{CH_4} = (k_M/k_{FT})([H]\alpha_1/k_{FT}[x]) \quad (8)$$

where $\alpha_1 = (k_g [CH_2]/(k_g[CH_2] + k_M[H])$ if it is assumed that the CH_2 intermediate is a chain growth monomer ($C_{n-1}H_{2n-1}$-s + CH_2-s -> C_nH_{2n+1} + 2s). Since the surface concentration of the CH_2 species is associated with the chain growth rate and chain termination rate constants (i.e. catalyst intrinsic property) and partial pressures of various reactants and products (process conditions), the formation of CH_4 is complicated and governed by intrinsic factors related to the catalyst as well as process conditions. Thus, the previously discussed asymmetric V-shaped CH_4 selectivity versus conversion patterns over different Fe-K catalysts shown in Figure 1 and Table 2 are likely consistent with this kinetic view, and suggest a rather complicated CH_4 formation process that is determined by both the nature of the catalyst and process conditions. It appears that the catalyst properties played a greater role relative to process conditions in controlling CH_4 formation at low conversion. On the other hand, process conditions had a greater influence on CH_4 formation at the high conversions for the low K containing catalyst.

The water produced by FTS could slightly change the CH_4 selectivity of the iron catalyst as well. Isotopic and water cofeeding studies [43-45] reported that indigenous water positively or negatively affected the FTS rate and CH_4 formation for cobalt catalyst, respectively, which was attributed to the water increasing surface active carbon species. Taking into account the negative role of water on CH_4 selectivity, a better explanation of the CH_4 selectivity trend is expected. Figure 3 shows the variation of P_{H_2O} with X_{CO} for the Fe-K catalysts. For the 1 and 2 K catalysts, volcano shaped P_{H_2O} versus X_{CO} curves were observed, peaking in the range of 40–50% CO conversion (0.07-0.075 MPa). The rapid increase in P_{H_2O} with CO conversion likely resulted in an additional contribution on reducing the CH_4 selectivity if the negative impact of water on CH_4 formation is considered. For the 3K and 5K catalysts, P_{H_2O} was significantly lower and increased almost linearly with increasing CO conversion over the entire range of conversion (Figure 3).

Thus, the increased P_{H_2O} partial pressure might slightly decrease CH_4 selectivity in the low CO conversion range for the 3K and 5K catalysts; above 50% CO conversion, the WGS reaction likely played a dominant role in adjusting CH_4 selectivity for the 3K catalyst. Nevertheless, the conditions did not greatly impact CH_4 selectivity with the 5K catalyst due to the dominant role of K on CO dissociation and chain growth.

The selectivity trends for the CH_4 and oxygenates as discussed above did not result from the iron phase changes occurring at different conversion levels. To confirm this, the 3K iron catalyst was selected to run at high (80%) and low (30%) CO conversion level for 192 h, respectively, with the other conditions being identical. The two used catalysts were characterized by Mössbauer spectroscopy, and the results are shown in Figure 4. Three phases of iron, i.e. χ-Fe_5C_2, ε'-carbide, and magnetite (Fe_3O_4), were detected in both samples and are represented by three blue sextets, two green sextets and one red sextet, respectively. Interestingly, the intensities of the three iron phases in the two spectra were similar; the composition was 49-56% magnetite, 5-6% ε'-$Fe_{2.2}C$ and 39-45% χ-Fe_5C_2; namely, the iron catalyst phases did not change significantly over a wide range of CO conversion. Since these iron phases were formed during FTS conditions as evident in the current and previous Mössbauer spectroscopy data, the observed CH_4 selectivity trends were likely caused by the CO conversion effect, but not the minor iron phase transformation during the reaction.

The XRD spectra of four reduced Fe-K catalysts are shown in Figure 5. All four reduced Fe-K catalysts show similar XRD patterns in the 2θ range of 25° - 85°. The two most intense reflections observed at 2θ of 35.5° and 43.5° represent the characteristic peak of Fe_3O_4 (PDF# 00-003-0863), while the small peak observed at 40 °C could be identified as Fe_2C_5 (PDF# 00-051-0997). The diffraction peak for the iron carbides expected to occur at 2θ = 42.6 ° 45° are not

observed in this study, which could be due to the effect of O passivation or air oxidation of the samples after the passivation. The intensity of the corresponding magnetite at 43.5 ^{o} in all cases are similar indicating similarly sized iron oxide species. To illustrate if K changed the size of iron carbide domains which are usually assumed to be FTS active sites, the crystal size of iron carbides at the characteristic peak at 40^{o} were calculated using the Scherrer equation. The iron carbides were estimated to be 20.5, 16.3, 15.0 and 17.1 nm for the reduced 1K, 2K, 3K and 5 K catalysts, respectively, which indicates that the iron carbide domain size did not change greatly with K loading. The XRD of the used iron catalysts for this study were not successfully obtained, since not enough sample was obtained after extraction. However, comparing the above XRD results with that of the used 3K catalyst reported previously [46], it is found the domain size of iron carbide for these reduced iron catalysts (15-21 nm) and the used 3K catalyst at 40^{o} (19.8 nm) are similar. Thus, the XRD results of the Fe-K catalysts is in line with the above discussed Mossbauer results, and suggests that the CO conversion effect played a dominant role in changing catalyst selectivity; moreover, the effect was affected by the K loading rather than the domain size.

Effect of CO conversion on oxygenate selectivity of Fe catalysts

Oxygenates are products of the FTS reaction with precipitated-iron based catalysts and can be upgraded to useful chemicals [19,47,48]. However, information about the effect of CO conversion on oxygenate selectivity is rather scarce. In this paper, we explored the changes in oxygenate selectivity and distribution with conversion and K loading in the 4–85% range. The oxygenates were found to be present in aqueous and oil phases of the iron catalysts (see Figure 6a-b). The water phase was generally comprised of up to C_5 oxygenates while detectable

amounts up to C_{17} were found in the oil phase. The amounts in both phases were quantified and summed for a comparison. Figure 7 depicts the change in oxygenate selectivity with CO conversion for all four Fe-K catalysts.

With the 3K catalyst at 260 ^{o}C, the oxygenate selectivity was low (i.e., ~0.5%) at 4% CO conversion; it increased rapidly with increasing CO conversion and reached 2.3% at 20% of CO conversion. After that point, it continued to increase to 2.7% at a slower rate up to ~50% CO conversion; the oxygenate selectivity then reversed its trend and decreased with further increases in CO conversion, dropping to 1.95% at 80% of CO conversion. On the 1 K and 2 K catalysts, the oxygenate selectivity displayed similar patterns, but the peak values of 2.9% and 2.2% occurred at 270 and 260 ^{o}C, respectively for 1 K; on the other hand, a peak value of 2.5% for 2 K at 260 ^{o}C was observed. Compared to the 3 K catalyst, the 1 K and 2 K catalyst displayed lower oxygenate selectivity at the same temperature (260 ^{o}C), with more oxygenate products being present in the aqueous phase. This is consistent with the finding of Dry et al. (i.e., for precipitated FeSiK) [47] that oxygenate formation was enhanced by increasing potassium content. Dictor and Bell [48] (using supported Fe_2O_3/K), Bukur et al. [26] (using precipitated FeCuK) and Ma et al. [19] (using supported FeCuK/AC) suggested that K promoter suppresses oxygenate and methanol formation. The different conclusions about the K effect on oxygenates in these studies might originate from using a different basis, for example, in the latter case, with the conclusion being made only on the basis of the water phase analysis, while the oxygenates in the oil phase were not considered. However, it must be noted that much higher K loadings (e.g., x = 5) did not result in additional increases in oxygenates. Furthermore, according to Figure 7, high temperature slightly suppressed oxygenate formation in the high conversion range, i.e. >50%.

The variation in oxygenate selectivity with CO conversion and K loading might suggest that different mechanisms operate for oxygenate versus hydrocarbon formation. It has been postulated that CO insertion is a chain growth path to form CH_3-CO or R-CO intermediates, which can be hydrogenated by H or OH groups to form different aldehydes, alcohols, acids, esters and oxygenates. Assuming this is the case, the fraction of CO insertion at low CO conversion could be low due to low contact time, resulting in low oxygenate selectivity. Increasing CO conversion appeared to promote CO insertion that favored oxygenate formation. However, a further increase in CO conversion (i.e., above 20-50%) likely hindered CO insertion but promoted CO adsorption and dissociation to form hydrocarbons. The result is consistent with the view that competitive reactions operate between oxygenate and hydrocarbon formation. However, given that iron carbides are active sites for hydrocarbon formation, the active sites for oxygenate formation on Fe-K catalysts remain unclear. It is speculated that some iron carbides, or more likely an interface between iron phases, could be responsible for oxygenate formation. On cobalt catalysts, while hydrocarbon formation is proposed to occur on metallic surface sites, oxygenate formation has been proposed to occur on cobalt carbides or a cobalt-promoter interface such as Co-Ce, or Co-Cu [49-51]. In the case of Co-Ce, cobalt has been proposed to be metallic whereas the ceria is a partially reduced oxide, where water and oxygenates are activated on ceria, with the metal assisting in H-transfer reactions. In one view, CO reacts with bridging OH groups on partially reduced ceria to form formates or a related species, which serves as an intermediate for molecular CO transfer from the support across the interface to the metal; this assists in terminating the growing hydrocarbon chains by molecular CO insertion. One might envision a similar scenario with iron, whereby iron carbide serves to promote H-transfer, with Fe_3O_4 serving as the partially reduced oxide. However, further research is needed

to test this hypothesis.

In light of oxygenate and hydrocarbon formation mechanisms as discussed above, a CO hydrogenation pathway for different products is illustrated in Figure 8.

Effect of CO conversion and K loading on oxygenate distribution

The representative oxygenate distribution obtained on the 1K and 3K catalysts is provided in Figure 9. C_1-C_5 alcohols were the main oxygenates detected for both Fe-K catalysts, varying from 0.5-8%, while 2-butanone, acid, acetone, and acetaldehyde propionaldehyde were lower (e.g., less than 0.5%). Among the oxygenates, the distribution of C_1-C_4 alcohols was 1-1.5%; 1.5-4.0%, 0.6-2.0% and 0.5-1.0% for the 1K catalyst and 0.5-1.0%, 1-8%, 1-2% for the 3K catalyst. Ethanol was the dominant alcohol for both catalysts and increased with CO conversion, especially for the 3K catalyst. It is speculated that the surface concentration of methyl (CH_3) groups on the catalyst surface was higher due to high K or high CO driving CO dissociation; this in turn leads to greater ethanol production than other alcohols by the CO insertion mechanism. The assumption is in line with a mechanistic study for oxygenate formation on iron catalysts using in-situ DRIFTS [52], which proposes that acetyl (CH_3CO) was the main chain growth monomer and hydrogenation of the monomer was a crucial step for oxygenate formation.

The total amount of oxygenates in the aqueous phase for the Fe-K catalysts was about 3-15% under typical FTS conditions. If 10-20% aqueous products are produced with FTS hydrocarbons on Fe-K catalysts, the low percentage of water still represents a significant amount of high value oxygenates being formed during FTS. For example, if an FTS plant has a capacity of 1 MT synfuels (HCs) per year, the plant would produce 3000 - 20,000 tons of alcohols each year in addition to synfuels. Thus, the current results highlight the significance of

utilizing XTL technology to convert coal, natural gas, or biomass to transportation fuels.

Combining C_1-C_5 oxygenates present in the water phase with the C_4-C_{17} oxygenates present in the oil phase of the iron FTS, a representative overall oxygenate distribution of the 3K catalyst is presented in Figure 10. Similar to the hydrocarbon distribution, the overall alcohol distribution of the 3 K catalysts follows the trend predicted by the ASF kinetic model quite well. The chain growth probability had a slight decrease with increasing CO conversion above 20%. The α values for the oxygenates and CO conversion for the 3 K catalyst were: 0.32 (4.3%), 0.79 (16.1%), 0.77 (34.5%), 0.75 (53.6%) and 0.72 (78%). This low α value is likely due to holdup of oxygenates in the liquid phase. This is consistent with increased hydrocarbon chain growth with increasing CO conversion. As previously mentioned, only C_1-C_8 oxygenates at various conversions for the 1 K catalyst were detected (results not shown), indicating low oxygenate chain growth on the 1 K catalyst relative to the 3K catalyst.

4. Conclusions

The effects of CO conversion on CH_4 selectivity were studied over four K promoted iron catalysts (i.e., 1K, 2K, 3K and 5K) using a 1 L CSTR. A wide range of CO conversion (i.e., 4-85%) was examined at 260-270 ^oC, 1.3 MPa, and $H_2/CO = 0.67$. The CH_4 selectivity versus CO conversion was found to display an asymmetric "V" shaped curve, with the lowest CH_4 selectivity occurring at ~50% CO in all cases. However, the CO conversion effect was suppressed remarkably with increasing K loading. At lower conversion levels (i.e., less than 50%), CH_4 selectivity exhibited a greater change (from 49% to 3%), and it depended on K loading. At higher conversions, greater than 50%, the changes were relatively smaller (from 20%

to 30%). From a kinetic point of view, the unique CH_4 selectivity trend highlights the complexity of CH_4 formation, which can be explained by the nature of the Fe-K catalyst and process conditions (e.g., CO conversion level). CH_4 selectivity decreased greatly from 5.2 to 1.9% with increasing K loading from 1 to 5K. The results suggest that (1) high K loading remarkably suppressed H_2 adsorption such that a hydrogen-lean environment was created, with H_2 pressure being a main factor to adjust CH_4 selectivity; (2) high K loading greatly promoted CO adsorption and dissociation and promoted chain growth.

The effect of CO conversion on oxygenate selectivity for the Fe-K catalysts was studied as well. The product spectrum of the Fe-K catalyst featured low oxygenate selectivity (i.e., less than 3%) that was comprised of mainly alcohols, with ethanol being the dominant alcohol. Up to C_{17} oxygenates were detected and followed an ASF distribution. The oxygenate selectivity versus CO conversion exhibited a volcano-shaped curve, and a maximum occurred in the range of 20-50% CO conversion. Up to 3K loading enhanced oxygenate formation and promoted oxygenate chain growth. The CO insertion mechanism was found to satisfactorily explain the oxygenate trend with CO conversion.

The Mossbauer and XRD results show that structural changes and particle size effects on the CO conversion effect were negligible.

Acknowledgments

This work was made possible by the Commonwealth of Kentucky. The authors are like to greatly thank G. Thomas for the ICP analyzing work and S. Hopps for the XRD experiment.

References

[1] A.P. Steynberg, M.E. Dry (eds.), Fischer-Tropsch Technology, Stud. Surf. Sci. Catal., 152, 2004, pp. 1–680.

[2] R. Overtoom, N. Fabricius, W. Leenhouts, Shell GTL, from Bench scale to World scale, in Advances in Gas Processing, Proceedings of the 1st Annual Gas Processing Symposium, (Eds.: H.E. Alfadala, G.V.R. Reklaitis, M.M. El-Halwagi), 10–12 January 2009, Doha, Qatar, 2009, pp. 378–386

[3] H.C. Heng, S. Idrus, J. Nat. Gas Chem. 13 (2004) 63–70.

[4] A.Y. Khodakov, Catal. Today 144 (2009) 251–257.

[5] D. A. Wood, C. Nwaoha, B.F. Towler, J. Nat. Gas Sci. Eng. 9 (2012) 196–208.

[6] D.B. Bukur, B. Todic, N. Elbashir, Catal. Today 275 (2016) 66–75.

[7] J. Xu, Y. Yang, Y.-W. Li, Fuel 152 (2015) 122-130.

[8] Z.Y. Liu, S.D. Shi, Y.W. Li, Chem. Eng. Sci. 65 (2010) 12–17.

[9] Significant coal-to-liquid project in production in Ningxia, http://www.china.org.cn/china/2016-12/29/content_40003229.htm

[10] Ø. Borg, S. Eri, E.A. Blekkan, S. Storsæter, H. Wigum, E. Rytter, A. Holmen, J. Catal. 248 (2007) 89-100.

[11] W. Ma, G. Jacobs, Y. Ji, T. Bhatelia, D.B. Bukur, S. Khalid, B.H. Davis, Top. Catal. 54 (2011) 757-767.

[12] D.B. Bukur, Z. Pan, W. Ma, G. Jacobs, B.H. Davis, Catal. Lett. 142 (2012) 1382-1387.

[13] J. Yang, G. Jacobs, T. Jermwongratanachai, V.R.R. Pendyala, W. Ma, D. Chen, A. Holmen, B.H. Davis, Catal. Lett. 144 (2014) 123-132.

[14] A.P. Raje, B.H. Davis, Catal. Today 36 (1997) 335-345.

[15] A.P. Raje, R.J. O'Brien, B.H. Davis, J. Catal. 180 (1998) 36.

[16] R.J. O'Brien, B.H. Davis, Catal. Lett. 94 (2004**)** 1-6.

[17] J. Yang, W.P. Ma, D. Chen, A. Holmen, B.H. Davis, Appl. Catal., A: Gen. 470 (2014) 250– 260.

[18] W. Ma, G. Jacobs, T.K. Das, C.M. Masuke, J. Kang, V.R.R. Pendyala, B.H. Davis, J.L.S. Klettlinger, C.H. Yen, Ind. Eng. Chem. Res. 53 (2014) 2157-2166.

[19] W. Ma, E.L. Kugler, D.B. Dadyburjor, Energy Fuels 21 (2007) 1832-1842.

[20] Y. Yang, H.-W. Xiang, Y.-Y. Xu, L. Bai, Y.-W. Li, Appl. Catal. A: Gen. 266 (2004) 181-194.

[21] B.H. Davis, Technology Development for Iron Fischer-Tropsch Catalysis, DOE final report, 1998.

[22] B.H. Davis, G. Jacobs, W. Ma, D. Sparks, K. Azzam, J.C. Mohandas, W. Shafer, V.R.R. Pendyala, Sensitivity of Fischer-Tropsch synthesis and water-gas shift catalysts to poisons from high-temperature high-pressure entrained-flow (EF) oxygen blown gasifier gasification of coal/biomass mixtures, DOE final report, 2011.

[23] V.R.R Pendyala, G. Jacobs, M.K. Gnanamani, Y.Hu, A. MacLennan, B.H. Davis, Appl. Catal. 495 (2015) 45–53.

[24] J.T. Scanion, D.E. Willis, J. Chromat. Sci. 23 (1985) 333.

[25] W.P. Ma, E.L. Kugler, D.B. Dadyburj et al. Energy Fuels 2011, 25, 1931–1938.

[26] D.B. Bukur, D. Mukesh, S.A. Patel, Ind. Eng. Chem. Res. 29 (1990) 194-204.

[27] H. Kolbel, Kalium als strucktureller und Energetischer Promoter in Eisenkatalysatoren. In Actes du Deuxieme Congres International de Catalyse; Technip: Paris, 1960; pp 2075-2099.

[28] M. E. Dry, T. Shingles, L.J. Boshoff, G.J. Oosthuizen, J. Catal. 1969, 15: 190-199.

[29] J.J. Venter, A.A. Chen, J. Phillips, M.A. Vannice, J.Catal. 1989, 119: 451-466.

[30] H. Arakawa, A.T. Bell, Ind. Eng. Chem. Process. Des. Dev. 1983, *22*, 97-103.

[31] C.H. Zhang, G.Y. Zhao, K.K. Liu, Y.Yang, H.W. Xiang, Y.W. Li, J.Mol. Catal. 2010, 328: 35-43.

[32] F. Fischer, H. Tropsch, Brennstoff Chem. 7 (1926) 97-104.

[33] R.C. Brady, R. Pettit, J. Am. Chem. Soc. 103 (1981) 1287-1289.

[34] H. Pichler, H. Schulz, Chem. Ing Tech. 42 (1970) 1162-1174.

[35] B. Todic, W.P. Ma, G. Jacobs, B.H. Davis, D.B. Bukur, Catal. Today 228 (2014) 32–39.

[36] R.B. Anderson, R.A. Friedel, H.H. Storch, J. Chem. Phys. 19 (1951) 313-319.

[37] B.H. Davis, Catal. Today 141 (2009) 25–33.

[38] P.M. Maitlis, R. Quyoum, H.C. Long, M.L. Turner, Appl. Catal., A: Gen. 186 (1999) 363-374.

[39] G.P. van der Laan, A.A.C.M. Beenackers, Appl. Catal. A: Gen. 193 (2000) 39–53.

[40] F.G. Botes, B.B. Breman, Ind. Eng. Chem. Res. 45 (2006) 7415-7426.

[41] M. Ojeda, R. Nabar, A.U. Nilekar, A. Ishikawa, M. Mavrikakis, E. Iglesia, J. Catal. 272 (2010) 287–297.

[42] L.P Zhou, X. Hao, J.H Gao, Y. Yang, B.S. Wu, J. Xu, Y.Y. Xu, Y.W. Li, Energy Fuels 25 (2011) 52–59.

[43] C.J. Bertole, C.A. Mims, G. Kiss, J. Catal. 210 (2002) 84–96.

[44] S. Loegdberg, M. Boutonnet, J.C. Walmsley, S. Jaeras, A. Holmen, E.A. Blekkan, Appl. Catal. A: Gen. 393 (2011) 109.

[45] W. Ma, G. Jacobs, D.E. Sparks, R.L. Spicer, B.H. Davis, J.L.S. Klettlinger, C.H. Yen, Catal. Today 228 (2014) 158-166.

[46] Ma, W.; Jacobs, G.; Thomas, G.A.; Shafer, W.D.; Sparks, D.E.; Hamdeh, H.H.; Davis, B.H., ACS Catalysis 5 (2015) 3124-3136.

[47] M.E. Dry in J.R. Anderson, M. Boudart (Eds.), Catalysis Science and Technology, Vol. 1, Springer-Verlag, New York, 1981, pp 175-183.

[48] R.A. Dictor, A.T. Bell, J. Catal. 97 (1986) 121-136.

[49] G.G. Volkova, T.M. Yurieva, L.M. Plyasova, M.I. Naumova, V.I. Zaikovskii, J. Mol. Catal. 158 (2000) 389-393.

[50] G. Prieto, S. Beijer, M.L. Smith, M. He, Y. Au, Z. Wang, D.A. Bruce, K.P.de Jong, J.J. Spivey, P.E.de Jongh, Angew. Chem. Intl. Ed. 53 (2014) 6397-6401.

[51] M.K. Gnanamani, M.C. Ribeiro, W.P. Ma, W. D. Shafer, G. Jacobs, U.M. Graham, B.H. Davis, Appl. Catal., A: Gen. 393 (2011) 17–23.

[52] W.Y. Mao, Q.W. Sun, W.Y. Ying, D.Y. Fang, Ranliao Huaxue Xuebao 41 (2013) 314-322.

Table 1. ICP analysis results for FeSiCuK catalysts

Catalyst	ICP analysis of Fe catalysts, atomic%			
	Fe	Si	Cu	K
100 Fe/5.1Si/2Cu/1.3K	100	5.3	1.8	1.2
100 Fe/5.1Si/2Cu/2 K	100	5.0	2.3	1.8
100 Fe/5.1Si/2Cu/3K	100	5.1	1.9	3.1
100 Fe/5.1Si/2Cu/5K	100	4.8	2.1	4.4

Table 2. CH_4 selectivity of 1K and 3K iron catalysts[(a)]

K loading	Time	X_{CO}	CH_4 selectivity, %		
x =	h	%	250 ºC	260 ºC	270 ºC
1.0	100-220	75	5.1	5.3	5.6
2.0	100-150	82	-	3.9	-
3.0	90-150	80	2.3	3.0	3.3
5.0	120-140	78	-	2.1	-

(a) Other reaction conditions: 1.31 Mpa, $H_2/CO = 0.67$, and 2.0-8.0 NL/g-cat/h.

Table 3. Selectivities of the iron catalysts with and without Cu[(a)]

Catalyst, %	TOS (hrs)	X_{CO} (%)	Selectivity, %			CO_2 selectivity, %
			CH_4	C_2-C_4	C_{5+}	
100Fe5.1Si1.25K	72-97	76.45	6.06	21.07	72.88	45.44
	477-501	48.35	5.45	23.82	70.72	45.51
100Fe5.1Si2Cu1.25K	121-335	74.65	5.78	21.80	72.43	47.70
	435-464	42.75	5.77	24.04	70.19	44.59

(a) Reaction conditions: 270 ^{o}C, 1.31 Mpa, H_2/CO = 0.67, and 2.0-19 NL/g-cat/h.

Table 4. Percentage change in CH_4 selectivity in the low and high CO conversion ranges

CO conversion level	CH_4 sel. change%			
	1K	2K	3K	5K
Low X_{CO} region (4-50%)	-48.8	-40	-25	-3.2
High X_{CO} region (50-85%)	30	30	33	20

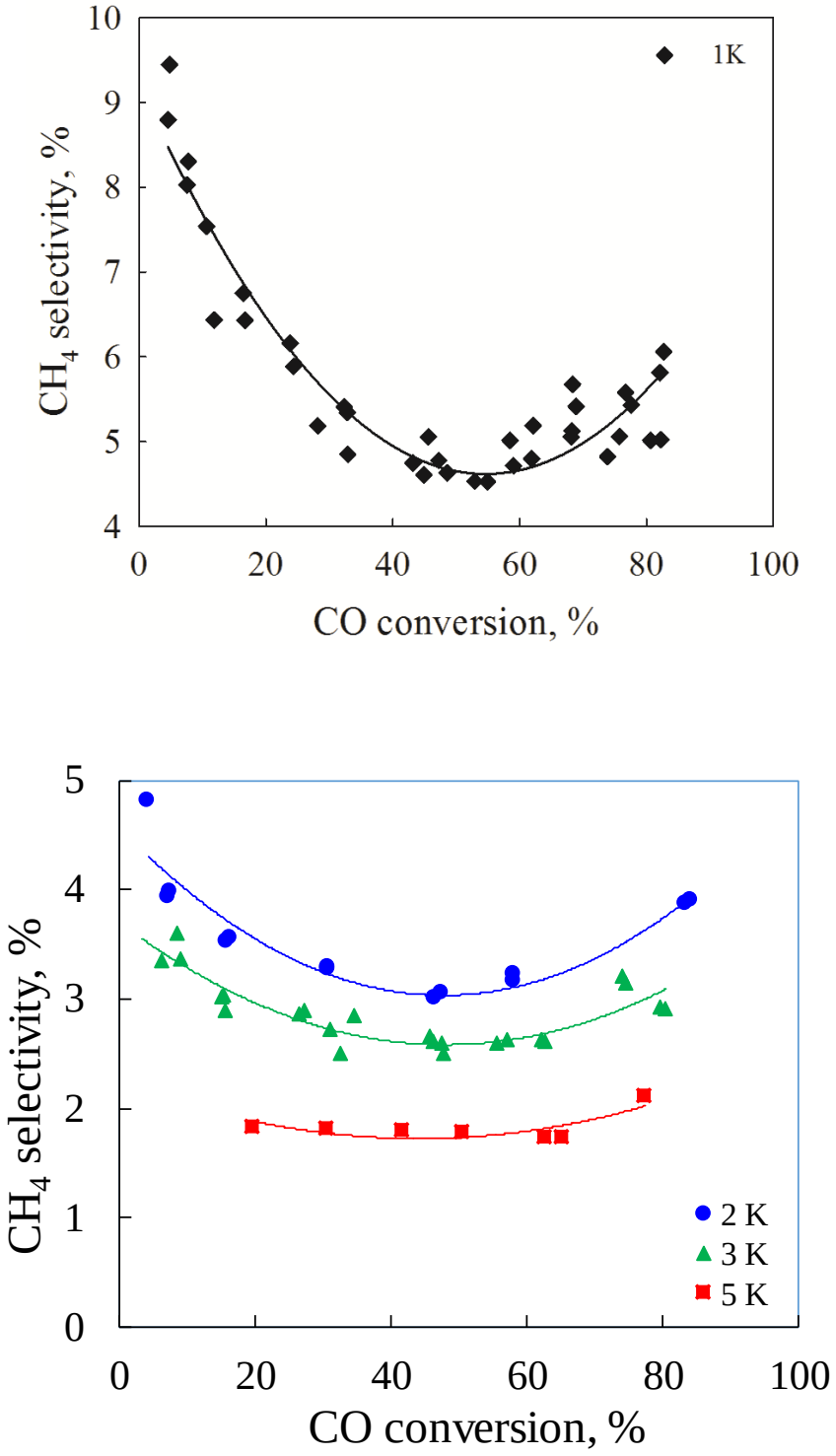

Figure 1. Change in CH_4 selectivity with CO conversion over 1 K catalyst (top) at 270 ^oC, 1.3 MPa, H_2/CO = 0.67, and 2K, 3K and 5K catalysts at 260 ^oC, 1.3 MPa, H_2/CO = 0.67.

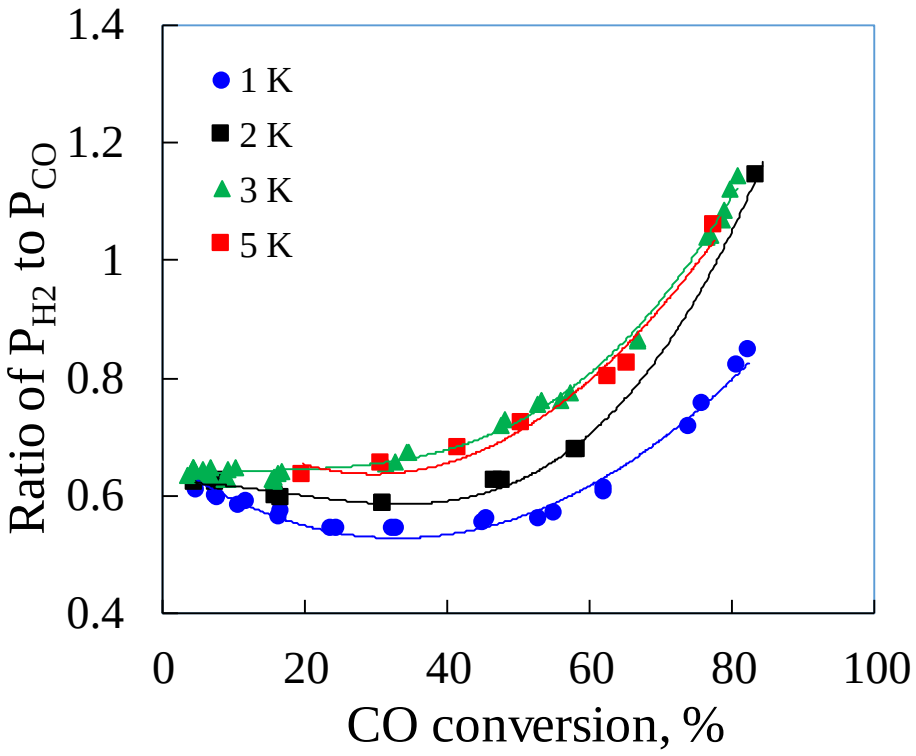

Figure 2. Change of P_{H_2O}/P_{CO} ratio in the reactor with CO conversion over 1 K catalyst (270 °C, 1.3 MPa, H_2/CO = 0.67) and 2K, 3K and 5 K catalysts (260 °C, 1.3 MPa, H_2/CO = 0.67).

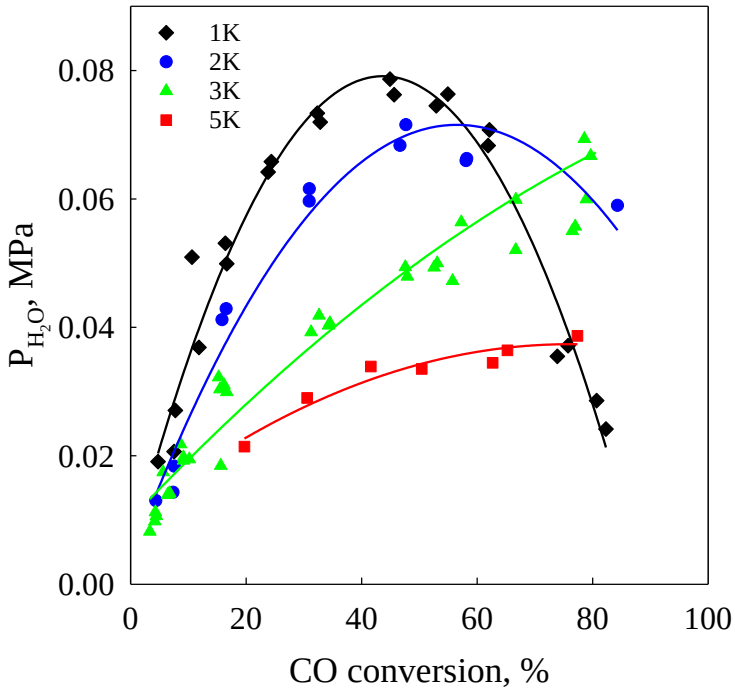

Figure 3. Change in P_{H_2O} in the reactor with CO conversion over 1 K catalyst (270 ^{o}C, 1.3 MPa, H_2/CO = 0.67) and 2K, 3K and 5 K catalyst (260 ^{o}C, 1.3 MPa, H_2/CO = 0.67).

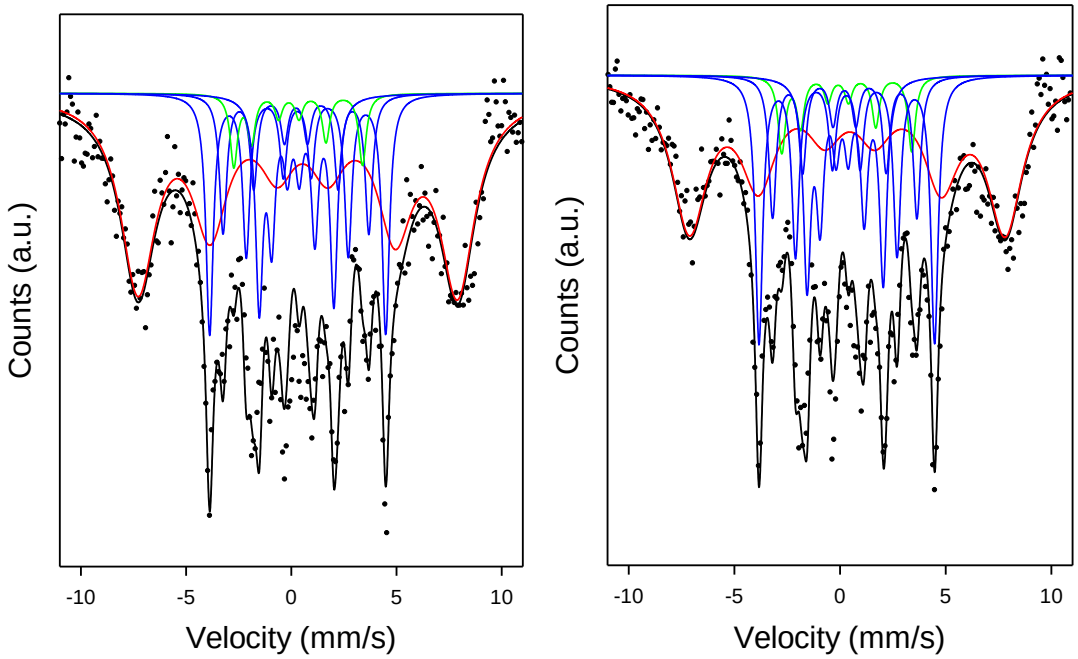

Figure 4. Mössbauer spectra of used 3 K catalyst at high (left) and low (right) conversions. Left: (X_{CO} = 80%): Fe_3O_4 (red line): 56%; χ–Fe_2C_5 (blue line): 38%; ε'–$Fe_{2.2}C$ (green line): 6% and low CO conversion (i.e., 30%). Right: (X_{CO} = 30%): Fe_3O_4 (red line): 49%; χ–Fe_2C_5 (blue line): 44%, ε'–$Fe_{2.2}C$ (green line): 7%. Other process conditions: 260 ^oC, H_2/CO = 0.67 and 1.3 MPa.

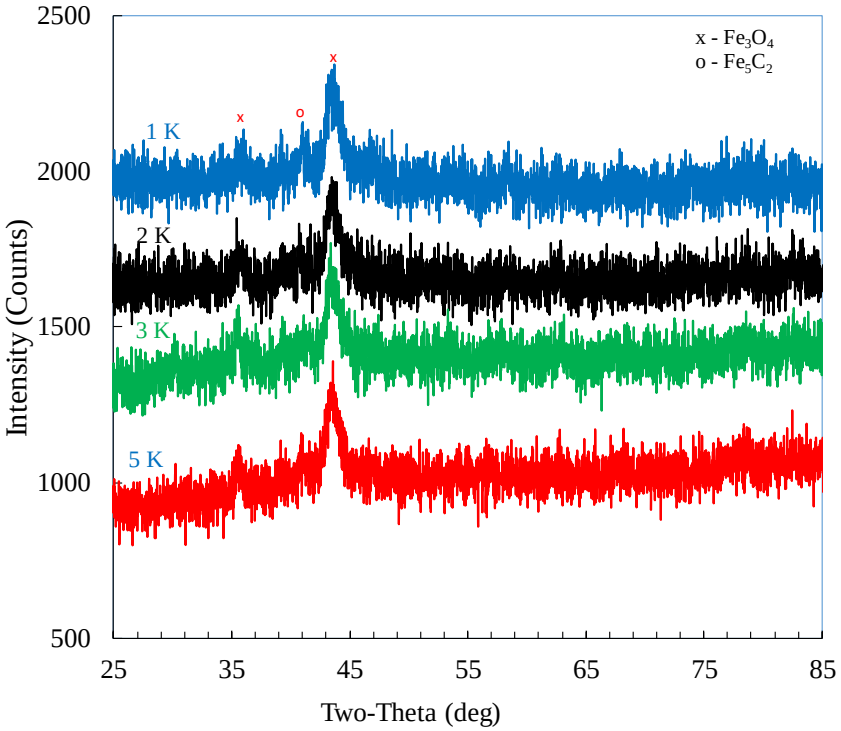

Figure 5. XRD spectra of four reduced Fe-K catalysts.

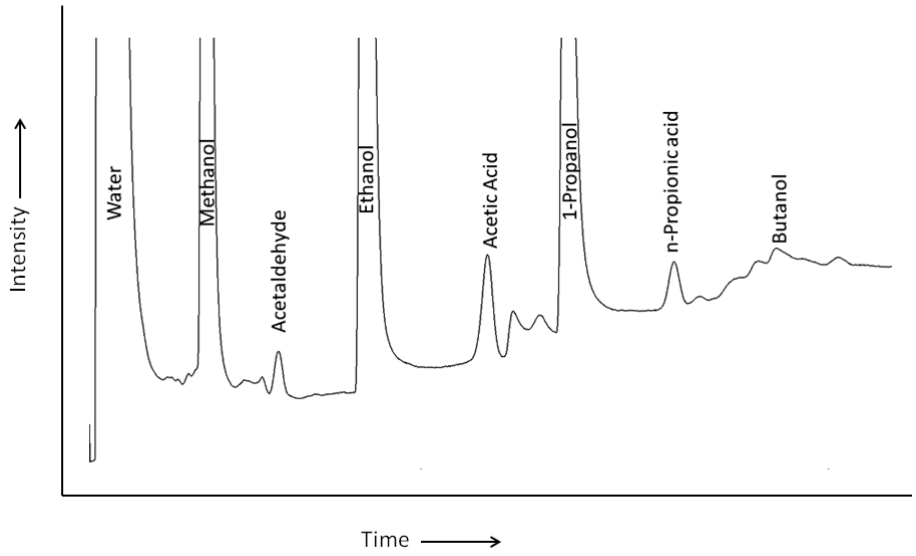

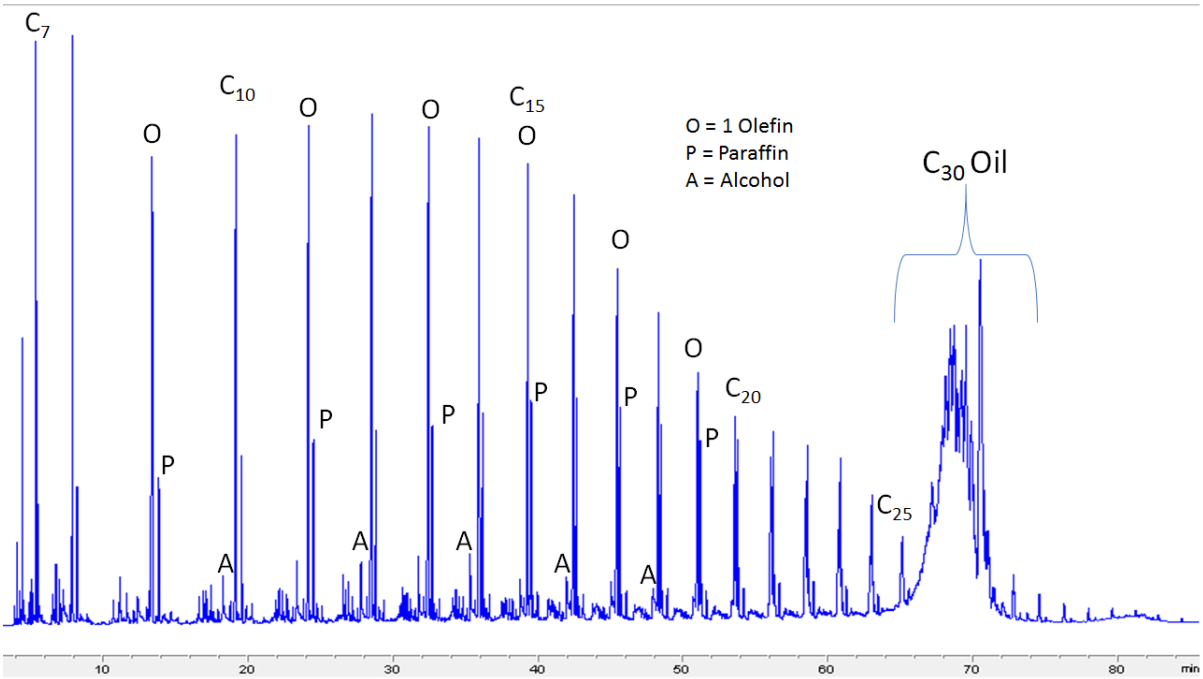

Figure 6. (a) GC trace of FT water product for 3K iron catalyst comprised of water and C_1-C_5 oxygenates. (b) GC trace of FT oil product for 3K iron catalyst comprised of C_4-C_{17} oxygenates.

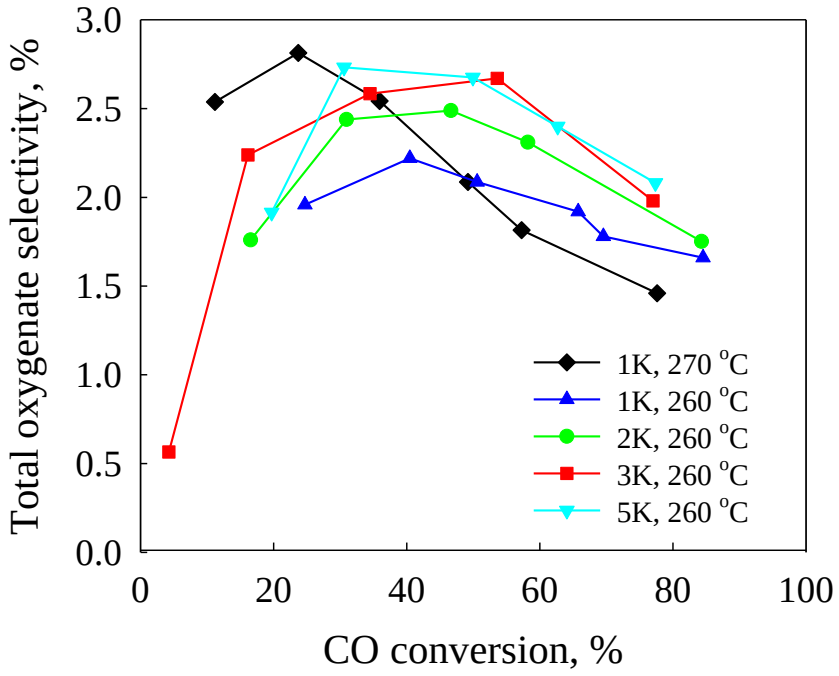

Figure 7. Oxygenate selectivity over 1K, 2K, 3K and 5K catalysts. Other process conditions: 1.3 MPa, $H_2/CO = 0.67$

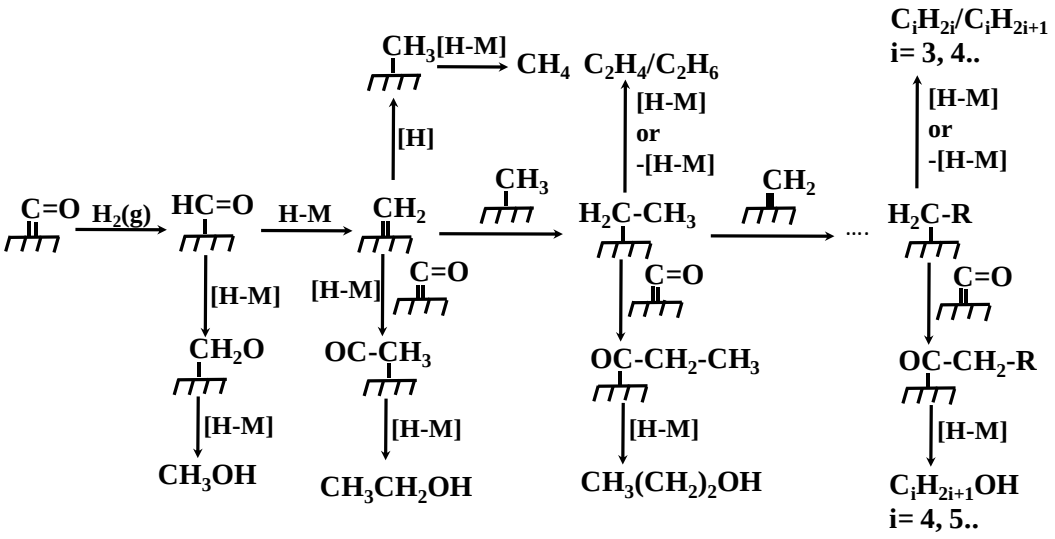

Figure 8. Proposed oxygenate and hydrocarbon formation pathway for Fe-K catalysts.

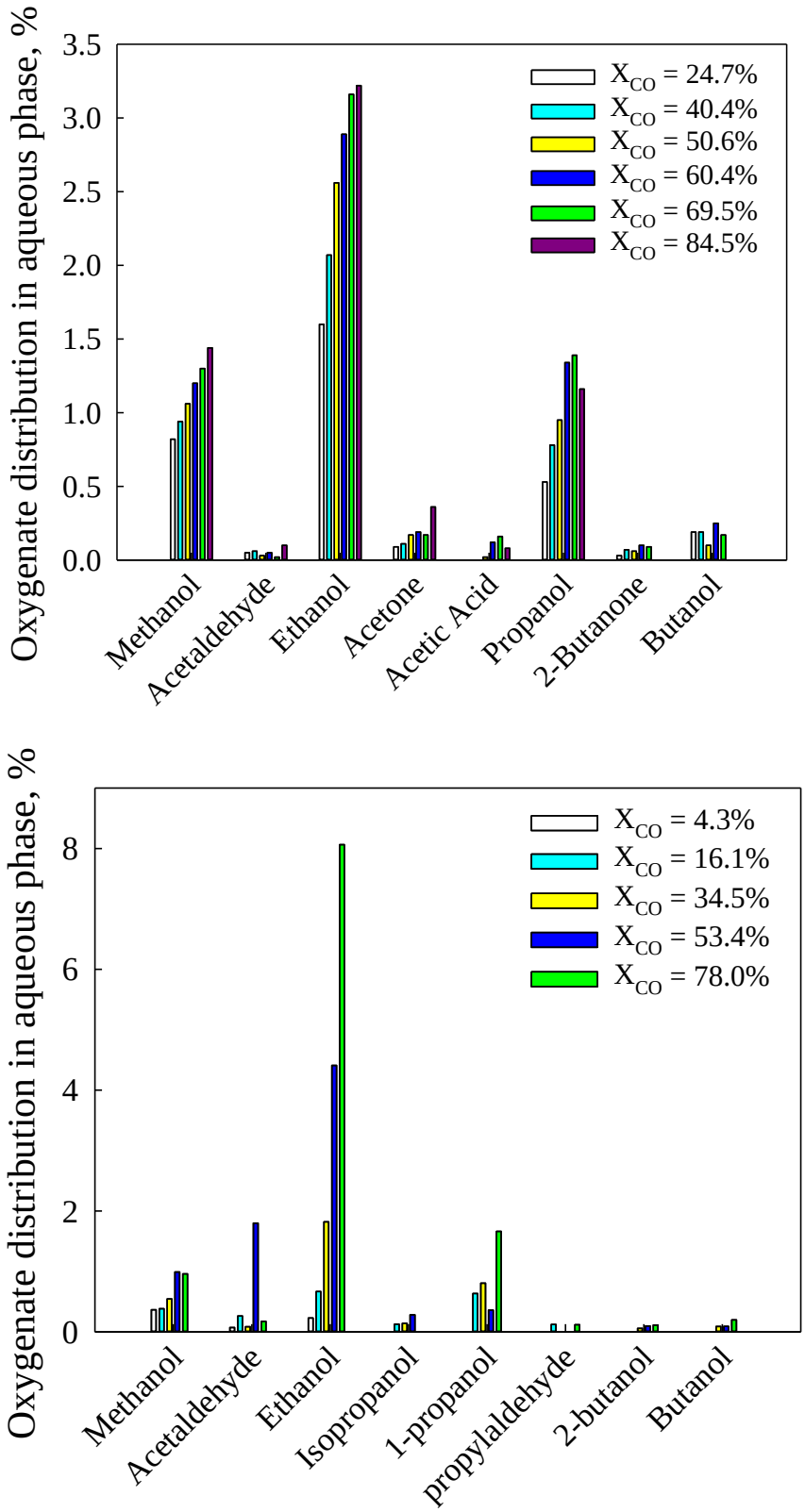

Figure 9. Oxygenate distributions as a function of conversion over 1K catalyst (top), and 3K catalyst (bottom). Other process conditions: 260 ^{o}C, 1.3 MPa, H_2/CO = 0.67.

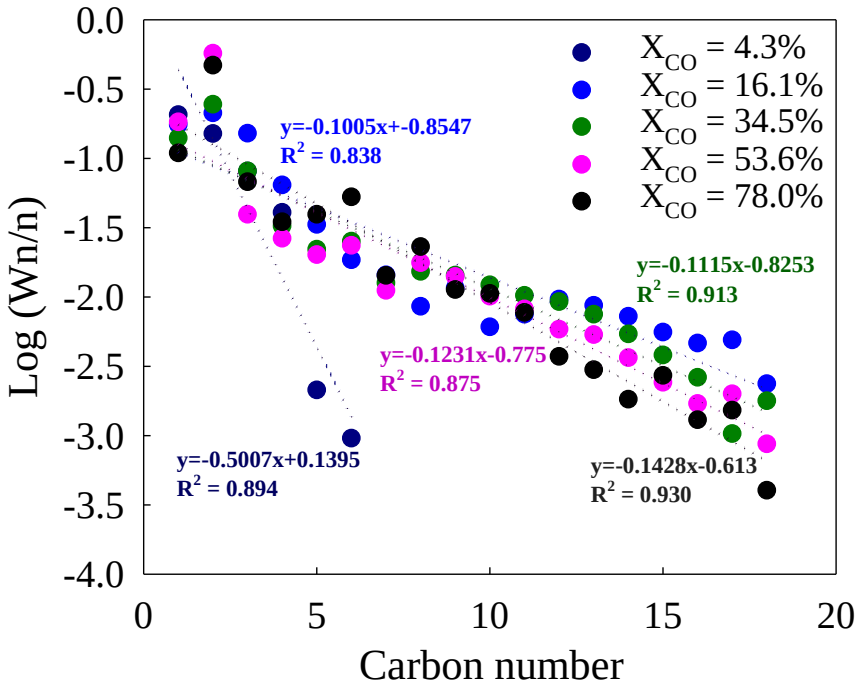

Figure 10. Overall oxygenate distribution of the 3 K catalyst following the ASF distribution. Other process conditions: 260 ^{o}C, 1.3 MPa, H_2/CO = 0.67.